

UC San Diego

UC San Diego Previously Published Works

Title

A Caged Enkephalin Optimized for Simultaneously Probing Mu and Delta Opioid Receptors

Permalink

<https://escholarship.org/uc/item/46h8x960>

Journal

ACS Chemical Neuroscience, 9(4)

ISSN

1948-7193

Authors

Banghart, Matthew R

He, Xinyi J

Sabatini, Bernardo L

Publication Date

2018-04-18

DOI

10.1021/acchemneuro.7b00485

Peer reviewed



HHS Public Access

Author manuscript

ACS Chem Neurosci. Author manuscript; available in PMC 2019 April 18.

Published in final edited form as:

ACS Chem Neurosci. 2018 April 18; 9(4): 684–690. doi:10.1021/acchemneuro.7b00485.

A Caged Enkephalin Optimized for Simultaneously Probing Mu and Delta Opioid Receptors

Matthew R. Banghart^{*,†,‡,iD}, Xinyi J. He[†], and Bernardo L. Sabatini^{*,‡}

[†]Division of Biological Sciences, Section on Neurobiology, University of California San Diego, La Jolla, California 92093, United States


[‡]Howard Hughes Medical Institute, Department of Neurobiology, Harvard Medical School, Boston, Massachusetts 02115, United States

Abstract

Physiological responses to the opioid neuropeptide enkephalin often involve both mu and delta opioid receptors. To facilitate quantitative studies into opioid signaling, we previously developed a caged [Leu⁵]-enkephalin that responds to ultraviolet irradiation, but its residual activity at delta receptors confounds experiments that involve both receptors. To reduce residual activity, we evaluated side-chain, N-terminus, and backbone caging sites and further incorporated the dimethoxy-nitrobenzyl moiety to improve sensitivity to ultraviolet light-emitting diodes (LEDs). Residual activity was characterized using an in vitro functional assay, and the power dependence and kinetics of the uncaging response to 355 nm laser irradiation were assayed using electrophysiological recordings of mu opioid receptor-mediated potassium currents in brain slices of rat locus coeruleus. These experiments identified *N*-MNVOC-LE as an optimal compound. Using ultraviolet LED illumination to photoactivate *N*-MNVOC-LE in the CA1 region of hippocampus, we found that enkephalin engages both mu and delta opioid receptors to suppress inhibitory synaptic transmission.

Graphical abstract

*Corresponding Authors. mbanghart@ucsd.edu. bernardo_sabatini@hms.harvard.edu.

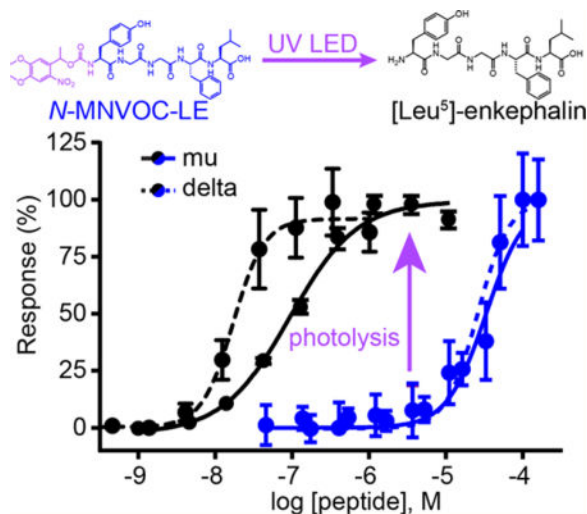
ORCID 

Matthew R. Banghart: 0000-0001-7248-2932

Author Contributions

M.R.B. and B.L.S. conceived of the project, designed experiments, and analyzed all data. M.R.B. designed the molecules, synthesized **5**, and performed the SEAP assays and electrophysiological experiments in locus coeruleus. X.J.H. performed and analyzed the data from the electrophysiological experiments in hippocampus. All authors commented on the manuscript and approved the final submission.

The authors declare no competing financial interest.



Keywords

Caged compounds; neuropeptides; opioid receptors; potassium channels; synaptic transmission; neurophysiology

Caged neurotransmitters are valuable reagents for probing chemical signaling in the nervous system. For example, the ability to precisely control the quantity, timing, and subcellular localization of neurotransmitter release with millisecond precision and submicron resolution has provided important insights into biophysical features of glutamatergic synaptic transmission in dendritic spines.^{1,2} In contrast, far less is known about neuromodulatory neurotransmitters, which activate G protein-coupled receptors (GPCRs) to tune aspects of cellular neurophysiology such as neuronal excitability and the probability of neurotransmitter release. Driving selective release of a specific neuromodulator in neural tissue can be extremely challenging, especially for neuropeptides, which are typically released as secondary neurotransmitters in response to poorly defined forms of sustained neuronal activation. The inability to control neuropeptide release has limited our ability to study neuropeptide signaling dynamics in a quantitative manner.

To address this issue, we previously developed photo-activatable analogues of the opioid neuropeptides [Leu⁵]-enkephalin (LE) and dynorphin A (1–8), which are among the most abundant endogenous ligands for mu, delta, and kappa opioid receptors (MOR, DOR, and KOR).³ In the mammalian brain, the opioid system mediates behavioral reinforcement and pain perception. MOR, in particular, is the target of several highly addicting opiate analgesics and there is great interest in understanding the neurophysiology of opioid signaling. By providing convenient, quantitative control over opioid release on the millisecond time scale, caged opioid neuropeptides have proven valuable for probing the spatiotemporal limits and molecular mechanisms of opioid receptor signaling in ex vivo brain tissue preparations such as brain slices.^{3–6}

However, these studies have thus far been limited to MOR, as our first-generation caged LE [(α -carboxy-2-nitrobenzyl)-Tyr¹]-[Leu⁵]-enkephalin (CYLE, **1**, Scheme 1), which contains

an α -carboxy-2-nitrobenzyl (CNB) caging group on the C-terminal tyrosine side-chain of LE, retains significant residual activity at DOR³ (Figure 1). As with other neuromodulators, opioid neuropeptide signaling is complicated by the propensity of a single ligand to activate multiple GPCR targets in a physiological concentration range, albeit with different affinities.⁷ This poses a key challenge when designing caged agonists, as the same ligand may exhibit different structure–activity relationships at each receptor such that a single caging strategy might not be equally effective across all receptor targets. Although the affinity of **1** is reduced <100-fold in comparison to LE at MOR and DOR, because LE activates DOR with ~10-fold higher affinity than MOR, concentrations of **1** required to saturate MOR upon photolysis (~1 μ M in this assay), partially activate DOR (Figure 1). This residual affinity for DOR in the caged form greatly limits the implementation of **1** in brain tissue, as many brain regions express both MOR and DOR.^{4,8}

Furthermore, although the CNB caging group responds well to high-power 355 nm laser irradiation, which excites the tail end of its absorbance spectrum, it is less responsive to UV-LEDs (UV light-emitting diodes) that emit wavelengths of 365 nm and longer. Compatibility with these LEDs is desirable as they are more affordable and convenient to implement than typical UV lasers. Thus, alternative caging groups that absorb at longer wavelengths may be optimal for use by most laboratories. An additional consideration is that many brain slice experiments rely on enhanced green fluorescent protein (eGFP) to enable targeted recording from genetically defined cell classes, which typically involves illumination with 450–490 nm light.⁴ Although long-wavelength caging groups are advantageous in many regards,^{9,10} for neurophysiology experiments involving eGFP, a caging group with a modest red shift is more suitable.

We herein report the generation of an optimized caged enkephalin that exhibits less residual affinity for DOR and improved compatibility with readily available UV-LEDs.

RESULTS AND DISCUSSION

Peptide caging is challenging due to the limited number of cageable amino acid side chains that are critical for receptor binding. LE (sequence: Tyr-Gly-Gly-Leu-Phe) only offers Tyr¹, which led us to consider caging the N- and C-termini as well as backbone amide nitrogen atoms. Backbone caging is particularly attractive, as in principle, every amino acid can be caged in this way. Methylation of opioid peptide backbone amides to improve stability to proteases, at least in some positions, still affords potent agonists (e.g., DAMGO), whereas at others it has been found to reduce activity at DOR.¹¹ Yet to what extent bulky aromatic caging groups might influence receptor binding is not clear. C-terminus extension, with fluorophores or other functional probes, has afforded several agonists that retain high potency, leading us away from this as a potential caging site.^{12–14} In contrast, a positively charged ammonium ion, fulfilled by the peptide N-terminus in enkephalin, makes a critical interaction with a conserved aspartic acid within the MOR and DOR binding sites,^{15,16} suggesting that masking this charge with a caging group may be a good approach.

We explored these alternative caging strategies with three new caged enkephalin derivatives (Scheme 1). We examined two backbone-caged derivatives: [*N*-NB-Gly²]-LE (**2**) and [*N*-

NB-Gly³]-LE (**3**), which contain a nitrobenzyl group on the amide nitrogen of either glycine. Although we aimed to explore the remaining backbone caging sites, they proved challenging to synthesize or exhibited poor stability during purification, most likely due to steric crowding between the caging group and adjacent bulky amino acid side chains.¹⁷ To mask the N-terminal ammonium ion, we examined *N*-(1-(2-nitrophenyl)-ethoxycarbonyl)-[Leu⁵]-enkephalin (*N*-NPEOC-LE, **4**), which incorporates a neutral carbamate linkage to a nitrophenethyl caging group. To determine how these caging strategies influence ligand potency, we compared their activities at MOR and DOR to LE and **1** in a live-cell functional assay using recombinant receptors expressed in human embryonic kidney cells (Figure 1a).³ Whereas **2** retained significant affinity at MOR, both **3** and **4** exhibited similar reductions in efficacy to **1**. At DOR, however, although both backbone-caged peptides closely resembled **1**, the N-terminally caged variant **4** showed a dramatic decrease in potency, indicating that the N-terminus is the most optimal caging site in the series.

Nonaryl-substituted nitrobenzyl-derived caging groups such as those employed in **1–4** poorly absorb photons at wavelengths emitted by low-cost UV-LEDs. Conveniently, incorporating alkoxy substituents at the 4- and 5-positions of the nitrobenzyl ring shifts the absorbance maximum to ~350 nm to afford facile excitation by 365–405 nm light with essentially no absorbance beyond 430 nm, the low range of the spectrum typically used for excitation of eGFP fluorescence. Based on our findings with the unsubstituted nitrobenzyl series, we evaluated the 4,5-dimethoxy substituted analogs of **1** and **4** that utilize the α -carboxy-6-nitroveratryl (CNV) and α -methyl-6-nitroveratryloxycarbonyl (MNVOC) caging groups, respectively. The residual activities of [(α -carboxy-6-nitroveratryl)-Tyr¹]-[Leu⁵]-enkephalin (CNV-Y-LE, **5**) and *N*-(α -methyl-6-nitroveratryloxycarbonyl)-[Leu⁵] enkephalin (*N*-MNVOC-LE, **6**) at MOR and DOR are presented in Figure 1b. As expected from this minimal change in caging group structure, the pharmacological profiles closely resembled those of the parent compounds, with **6** maintaining a dramatic reduction in activity at DOR. These results of this pharmacological characterization are presented in Table 1.

We characterized the performance of these peptides at endogenous opioid receptors in neurons with whole-cell recordings of currents carried by MOR-activated G protein-activated inward rectifier K⁺ (GIRK) channels in brain slices of rat locus coeruleus (LC). Although LC neurons do not express DOR, the MOR-activated GIRK currents provide a sensitive assay of receptor activation with high temporal resolution. Using **1**, we previously found that enkephalin photorelease produces large outward GIRK currents with an activation time constant of several hundred milliseconds.³ We excluded **2** from this analysis due to its significant residual activity at MOR. Each compound was bath circulated at a concentration of 10 μ M and photoreleased using a 50 ms flash of collimated 355 nm laser irradiation with the recorded cell body positioned at the center of a $12 \times 10^3 \mu\text{m}^2$ field. To functionally probe the photoefficiency of release, we measured the currents evoked by three different power levels: 10, 30, and 100 mW (Figure 2a, b). This comparison revealed that all compounds afforded robust, light-evoked GIRK currents in this power range. Interestingly, whereas the backbone-caged derivative **3** produced smaller peak currents in response to 100 mW illumination than the other compounds, the CNV-tyrosine-caged variant **5** afforded larger

responses at lower power levels, suggesting an enhanced overall quantum efficiency compared to the other peptides.

Phenol release from CNB cages¹⁸ and backbone amide release from NB cages¹⁹ can proceed with microsecond kinetics, which is much faster than the time scale of MOR-mediated GIRK activation. In contrast, photorelease of carbamate-masked amines proceeds on the millisecond time scale as a result of the two-step, decarboxylative photorelease mechanism.^{20,21} To determine how the different caging strategies influence the temporal precision of opioid receptor photoactivation, we compared the kinetics of GIRK activation in response to 100 mW illumination (Figure 2c, d). In each case, the rising phase of the light-evoked current was well fit with a monoexponential, whose time constant reflects the time course of GIRK activation. This comparison revealed that, whereas photolysis of **1** and **5** activated GIRKs with similarly fast kinetics, photoactivation with **3**, **4**, and **6** proceeded ~1.5-fold more slowly (τ_{on} (s): (**1**) 0.233 ± 0.022 , (**3**) 0.424 ± 0.032 , (**4**) 0.379 ± 0.03 , (**5**) 0.245 ± 0.03 , (**6**) 0.434 ± 0.031). Although the apparent rates of photorelease for **3**, **4**, and **6** were somewhat slower than expected, in all cases, the light-evoked currents peaked within 1–2 s of the light flash onset.

Taken together these analyses point to **6** as the most optimal compound for probing MOR and DOR simultaneously in brain slice experiments. Although the rate of receptor photoactivation was slightly slower than for tyrosine-caged analogues **1** and **5**, it provided large photocurrents in response to 355 nm irradiation, an absorbance spectrum that extends beyond 400 nm and most critically, it was highly inactive at DOR prior to photolysis.

We therefore further examined **6** in brain slices of mouse hippocampus, where both MOR and DOR have been implicated in the regulation of inhibitory synaptic transmission,⁸ using a 365 nm UV-LED to drive photolysis. Whole-cell voltage clamp recordings were obtained from pyramidal neurons in the CA1 region and pairs of inhibitory postsynaptic currents (IPSCs) were evoked electrically (Figure 3a). Under these conditions, bath application of LE (6 μM) strongly suppressed inhibitory synaptic transmission (Figure 3a, b). This was accompanied by an increase in the amplitude of the second IPSC relative to the first (the paired pulse ratio, PPR), which indicates a reduction in neurotransmitter release probability (Figure 3c). In contrast, **6** (6 μM) had no effect when added to the bath (Figure 3b), consistent with its low residual activity at MOR and DOR. However, a 50 ms light flash applied 2 s before electrical stimulation caused a dramatic, transient reduction in IPSC amplitude that lasted for just over 1 min (Figure 3d, e). Similar to bath application of LE, this suppression of synaptic transmission was accompanied by an increase in the PPR (Figure 3f). Repeated application of the light stimulus every 5 min revealed that the uncaging response was stable and highly reproducible for at least an hour (Figure 3e, g).

Having established that **6** cleanly provides large uncaging responses, we asked if this suppression of inhibition is indeed mediated by both MOR and DOR. After obtaining a baseline uncaging response consisting of three uncaging events, highly selective antagonists of either MOR (CTOP, 1 μM) or DOR (TIPP-Psi, 1 μM) were applied to the bath (Figure 3g). Whereas CTOP or TIPP-Psi alone blocked about half of the photolysis-driven IPSC suppression, the presence of both antagonists completely abolished it (Figure 3g, h).

Together, these results indicate that both MOR and DOR contribute to the actions of LE on inhibitory synapses in the CA1 region of hippocampus and that our optimized derivative *N*-MNVOC-LE (**6**) is a suitable probe for studying the mixed actions of LE at opioid receptors in brain tissue.

The low residual activity and high sensitivity to 365 nm UV-LED illumination make *N*-MNVOC-LE (**6**) a powerful probe for probing the molecular, cellular, and synaptic mechanisms of enkephalinergic modulation in the nervous system. Future efforts will aim to preserve these properties while improving the kinetics of photorelease and providing sensitivity to two-photon excitation.

METHODS

Chemical Synthesis and Characterization

High-resolution mass spectrometry data were obtained at the UCSD Chemistry and Biochemistry Mass Spectrometry Facility on an Agilent 6230 time-of-flight mass spectrometer (TOFMS). All compounds were purified by reverse-phase HPLC to >99% purity, used as mixtures of diastereomers, and found to be stable in the dark for at least 24 h in phosphate-buffered saline at pH 7.2.

H-(α -Carboxynitrobenzyl)Tyr-Gly-Gly-Phe-Leu-OH (1)—Compound **1** was synthesized by PepTech Corp. by solid-phase peptide synthesis using protected CNB-tyrosine.^{3,18} HRMS (ESI) *m/z* calcd for C₃₆H₄₃N₆O₁₁ [MH]⁺ 735.2984, found 735.2980.

H-Tyr-(*N*-nitrobenzyl)Gly-Gly-Phe-Leu-OH (2)—Compound **2** was synthesized by AmbioPharm, Inc. via solid phase peptide synthesis using protected *N*-nitrobenzyl-glycine. HRMS (ESI) *m/z* calcd for C₃₅H₄₃N₆O₉ [MH]⁺ 691.3086, found 691.3089.

H-Tyr-Gly-(*N*-nitrobenzyl)Gly-Phe-Leu-OH (3)—Compound **3** was synthesized by AmbioPharm, Inc. in the same way as **2**. HRMS (ESI) *m/z* calcd for C₃₅H₄₃N₆O₉ [MH]⁺ 691.3086, found 691.3080.

(*N*-(1-(2-Nitrophenyl)ethoxy)carbonyl)Tyr-Gly-Gly-Leu-OH (4)—Compound **4** was synthesized by PepTech Corp. via solid phase peptide synthesis using ((1-(2-nitrophenyl)ethoxy)carbonyl)-L-tyrosine, which was accessed from 1-(2-nitrophenyl)ethanone. HRMS (ESI) *m/z* calcd for C₃₇H₄₅N₆O₁₁ [MH]⁺ 749.3141, found 749.3136.

H-(α -Carboxy-6-nitroveratryl)Tyr-Gly-Gly-Phe-Leu-OH (5)—Room lights were covered with Roscolux Canary Yellow #312 film (Rosco Laboratories). (*tert*-Butoxycarbonyl)-Tyr-Gly-Gly-Phe-Leu-OH (50 mg, 76 μ mol American Peptide Company) was dissolved in DMF (300 μ L) in an amber vial under argon gas, cooled on ice, and treated with NaH (3.6 mg, 150 μ mol) in DMF (300 μ L) in portions, prior to dropwise addition of 2-(trimethylsilyl)ethyl 2-bromo-2-(4,5-dimethoxy-2-nitrophenyl)acetate (32 mg, 76 μ mol, Shanghai Medicilon Inc.) in DMF (160 μ L). The reaction was warmed to room temperature and stirred for 19 h followed by the addition of 10% citric acid (100 μ L). The solvent was

removed in vacuo, triturated with hexanes, and treated with 60% TFA/dichloromethane (2 mL) for 3 h. The solvent was removed in vacuo and the product was purified by reverse-phase HPLC to yield **5** (21 mg, 23 μ mol, 30% overall yield) as an off-white residue. HRMS (ESI) m/z calcd for $C_{38}H_{47}N_6O_{13}$ [MH]⁺ 795.3196, found 795.3194.

N-(α -Methyl-6-nitroveratryloxycarbonyl)Tyr-Gly-Gly-Leu-OH (6)—Compound **6** was prepared by Shanghai Medicilon Inc. by treating [Leu⁵]-enkephalin with the succinyl carbonate of 1-(4,5-dimethoxy-2-nitrophenyl)ethanol. HRMS (ESI) m/z calcd for $C_{39}H_{49}N_6O_{13}$ [MH]⁺ 809.3352, found 809.3351.

Secreted Alkaline Phosphatase (SEAP) Assay

Dose–response curves were obtained as previously described.³

Brain Slice Preparation

Animal handling protocols were approved by the Harvard Standing Committee on Animal Care and the UC San Diego Institutional Animal Care and Use Committee. For measuring K⁺ currents (Figure 2), brain slices of rat LC were prepared as previously described.³ Briefly, postnatal day 12–22 Sprague–Dawley rats were anesthetized with isoflurane and killed, and the brain was removed, blocked, and mounted in a VT1000S vibratome (Leica Instruments). Horizontal slices (240 μ m) were prepared in ice-cold choline-ACSF containing (in mM) 25 NaHCO₃, 1.25 NaH₂PO₄, 2.5 KCl, 7 MgCl₂, 25 glucose, 1 CaCl₂, 110 choline chloride, 11.6 ascorbic acid, and 3.1 pyruvic acid, equilibrated with 95% O₂/5% CO₂. Slices were transferred to a holding chamber containing oxygenated artificial cerebrospinal fluid (ACSF) containing (in mM) 127 NaCl, 2.5 KCl, 25 NaHCO₃, 1.25 NaH₂PO₄, 2 CaCl₂, 1 MgCl₂, and 25 glucose, osmolarity 307. Slices were incubated at 32 °C for 30–45 min and then left at room temperature until recordings were performed. For measurements of synaptic transmission (Figure 3), horizontal slices (300 μ m) of hippocampus were prepared from postnatal day 15–25 C57/Blk6 mice using the same method.

Electrophysiology

All recordings were performed within 5 h of slice cutting in a submerged slice chamber perfused with ACSF warmed to 32 °C and equilibrated with 95% O₂/5% CO₂. Whole-cell voltage clamp recordings were made with an Axopatch 700B amplifier (Axon Instruments). Data were filtered at 3 kHz, sampled at 10 kHz, and acquired using National Instruments acquisition boards and a custom version of ScanImage written in MATLAB (Mathworks). Cells were rejected if holding currents exceeded –200 pA or if the series resistance (<25 M Ω) changed during the experiment by more than 20%. For recordings measuring K⁺ currents in rat LC neurons (Figure 2), patch pipets (open pipet resistance 1.6–2.2 M Ω) were filled with an internal solution containing (in mM) 135 KMeSO₄, 5 KCl, 5 HEPES, 1.1 EGTA, 4 MgATP, 0.3 Na₂GTP, and 10 Na₂-phosphocreatine (pH 7.25, 286 mOsm/kg). Cells were held at –55 mV, and synaptic transmission was blocked with the addition to the ACSF of 2,3-dihydroxy-6-nitro-7-sulfamoyl-benzo(*f*)quinoxaline (NBQX; 10 μ M), *R,S*-3-(2-carboxypiperazin-4-yl)propyl-1-phosphonic acid (CPP; 10 μ M), and picrotoxin (10 μ M). For recordings measuring inhibitory synaptic transmission in mouse hippocampus (Figure 3), patch pipets (2.8–3.5 M Ω) were filled with an internal solution containing (in mM) 135

CsMeSO₃, 10 HEPES, 1 EGTA, 3.3 QX-314 (Cl⁻ salt), 4 Mg-ATP, 0.3 Na-GTP, and 8 Na₂-phosphocreatine (pH 7.3, 295 mOsm/kg). Cells were held at 0 mV to produce outward currents. Excitatory transmission was blocked by the addition to the ACSF of NBQX (10 μM) and CPP (10 μM). To electrically evoke IPSCs, stimulating electrodes pulled from theta glass with ~5 μm tip diameters were placed at the border between stratum pyramidale and stratum oriens nearby the recorded cell (~50–150 μm) and a two brief pulses (0.5 ms, 50–300 μA, 50 ms interval) were delivered every 20 s. NBQX was obtained from HelloBio; CPP, picrotoxin, and D-Pen-Cys-Tyr-D-Trp-Orn-Thr-Pen-Thr-NH₂ (CTOP, 1 μM) were from Tocris; H-Tyr-Tic(CH₂NH)-Phe-Phe-OH (TIPP-Psi, 1 μM) was custom synthesized by RS Synthesis; and [leu⁵]-enkephalin (LE, 1 μM) was obtained from Sigma-Aldrich.

UV Photolysis

In LC, uncaging was carried out using 50 ms flashes of collimated full-field illumination with a 355 nm laser, as previously described.³ Light powers in the text correspond to measurements of a 10 mm diameter collimated beam at the back aperture of the objective. In hippocampus, uncaging was achieved using 50 ms flashes of full-field illumination from the 365 nm-UV channel of a pE-300^{white} LED (CoolLED) reflected through a 60× LUMPLANFL 1.0 NA objective (Olympus) on SliceScope Pro 6000 microscope (Scientifica) with a 405 nm long-pass dichroic mirror (Di02-R405-25×36, Semrock) mounted in the fluorescence turret. Light power was set to 5 mW in the sample plane (~120 mW of an ~20 mm diameter “beam” at the back aperture).

Data Analysis

SEAP data were fit using sigmoidal variable-slope nonlinear regression in GraphPad Prism (GraphPad Software). Electrophysiology data were analyzed in Igor Pro (Wavemetrics). Peak current amplitudes were calculated by averaging over a 200 ms (LC) or 2 ms (hippocampus) window around the peak. Activation time constants were calculated by fitting the rising phases of light-evoked currents to an exponential function. To determine magnitude of modulation by enkephalin uncaging (%IPSC suppression), the IPSC peak amplitude immediately after a flash was divided by the average peak amplitude of the three IPSCs preceding the light flash. The effects of drugs on IPSC suppression were calculated as the average %IPSC suppression by the three light flashes applied 10, 15, and 20 min after drug addition. Summary values were reported as mean ± SEM and were compared to each other using either the Mann–Whitney U test or Wilcoxon’s paired sign-ranked test. *P* values smaller than 0.05 were denoted with an asterisk.

Acknowledgments

We would like to thank Ruchir C. Shah and Nicole C. Wong for technical support, Shay Q. Neufeld and John T. Williams for performing pilot electrophysiology experiments, Luke D. Lavis for facilitating the synthesis of **5**, the ICCB-Longwood Screening Facility for access to plate readers, and Steven D. Liberles for SEAP assay plasmids.

Funding

This work was supported by the Howard Hughes Medical Institute (to B.L.S.), the National Institute of Mental Health (Grant R01 MH085498, to B.L.S.), the National Institute on Drug Abuse (Grant K99/R00 DA034648, to M.R.B.), and the National Institute of General Medical Sciences (T32 GM007240 to X.J.H.).

References

1. Bloodgood BL, Sabatini BL. Regulation of synaptic signalling by postsynaptic, non-glutamate receptor ion channels. *J. Physiol.* 2008; 586:1475–1480. [PubMed: 18096597]
2. Colgan LA, Yasuda R. Plasticity of Dendritic Spines: Subcompartmentalization of Signaling. *Annu. Rev. Physiol.* 2014; 76:365–385. [PubMed: 24215443]
3. Banghart MR, Sabatini BL. Photoactivatable Neuropeptides for Spatiotemporally Precise Delivery of Opioids in Neural Tissue. *Neuron.* 2012; 73:249–259. [PubMed: 22284180]
4. Banghart MR, Neufeld SQ, Wong NC, Sabatini BL. Enkephalin Disinhibits Mu Opioid Receptor-Rich Striatal Patches via Delta Opioid Receptors. *Neuron.* 2015; 88:1227–39. [PubMed: 26671460]
5. Williams JT. Desensitization of Functional μ -Opioid Receptors Increases Agonist Off-Rate. *Mol. Pharmacol.* 2014; 86:52–61. [PubMed: 24748657]
6. Banghart MR, Williams JT, Shah RC, Lavis LD, Sabatini BL. Caged naloxone reveals opioid signaling deactivation kinetics. *Mol. Pharmacol.* 2013; 84:687–95. [PubMed: 23960100]
7. Toll L, Berzetei-Gurske IP, Polgar WE, Brandt SR, Adapa ID, Rodriguez L, Schwartz RW, Haggart D, O'Brien A, White A, Kennedy JM, Craymer K, Farrington L, Auh JS. Standard binding and functional assays related to medications development division testing for potential cocaine and opiate narcotic treatment medications. *NIDA Res. Monogr.* 1998; 178:440–66. [PubMed: 9686407]
8. Lupica CR. Delta and mu enkephalins inhibit spontaneous GABA-mediated IPSCs via a cyclic AMP-independent mechanism in the rat hippocampus. *J. Neurosci.* 1995; 15:737–49. [PubMed: 7823176]
9. Olson JP, Banghart MR, Sabatini BL, Ellis-Davies GCR. Spectral evolution of a photochemical protecting group for orthogonal two-color uncaging with visible light. *J. Am. Chem. Soc.* 2013; 135:15948–54. [PubMed: 24117060]
10. Amatrudo JM, Olson JP, Agarwal HK, Ellis-Davies GCR. Caged compounds for multichromic optical interrogation of neural systems. *Eur. J. Neurosci.* 2015; 41:5–16. [PubMed: 25471355]
11. Rochon K, Proteau-Gagné A, Bourassa P, Nadon J-F, Côté J, Bournival V, Gobeil F, Guérin B, Dory YL, Gendron L. Preparation and Evaluation at the Delta Opioid Receptor of a Series of Linear Leu-Enkephalin Analogues Obtained by Systematic Replacement of the Amides. *ACS Chem. Neurosci.* 2013; 4:1204–1216. [PubMed: 23650868]
12. Fournie-Zaluski MC, Gacel G, Roques BP, Senault B, Lecomte JM, Malfroy B, Swerts JP, Schwartz JC. Fluorescent enkephalin derivatives with biological activity. *Biochem. Biophys. Res. Commun.* 1978; 83:300–5. [PubMed: 697818]
13. Arttamangkul S, Alvarez-Maubecin V, Thomas G, Williams JT, Grandy DK. Binding and internalization of fluorescent opioid peptide conjugates in living cells. *Mol. Pharmacol.* 2000; 58:1570–80. [PubMed: 11093798]
14. Lee TT, Williams RE, Fox CF. Photoaffinity inactivation of the enkephalin receptor. *J. Biol. Chem.* 1979; 254:11787–90. [PubMed: 227880]
15. Manglik A, Kruse AC, Kobilka TS, Thian FS, Mathiesen JM, Sunahara RK, Pardo L, Weis WI, Kobilka BK, Granier S. Crystal structure of the μ -opioid receptor bound to a morphinan antagonist. *Nature.* 2012; 485:321–326. [PubMed: 22437502]
16. Granier S, Manglik A, Kruse AC, Kobilka TS, Thian FS, Weis WI, Kobilka BK. Structure of the δ -opioid receptor bound to naltrindole. *Nature.* 2012; 485:400–404. [PubMed: 22596164]
17. Johnson ECB, Kent SBH. Synthesis, stability and optimized photolytic cleavage of 4-methoxy-2-nitrobenzyl backbone-protected peptides. *Chem. Commun.* 2006:1557.
18. Sreekumar R, Ikebe M, Fay FS, Walker JW. Biologically active peptides caged on tyrosine. *Methods Enzymol.* 1998; 291:78–94. [PubMed: 9661146]
19. Tatsu Y, Nishigaki T, Darszon A, Yumoto N. A caged sperm-activating peptide that has a photocleavable protecting group on the backbone amide. *FEBS Lett.* 2002; 525:20–4. [PubMed: 12163154]
20. Rossi FM, Margulis M, Tang CM, Kao JP. N-Nmoc-L-glutamate, a new caged glutamate with high chemical stability and low pre-photolysis activity. *J. Biol. Chem.* 1997; 272:32933–9. [PubMed: 9407072]

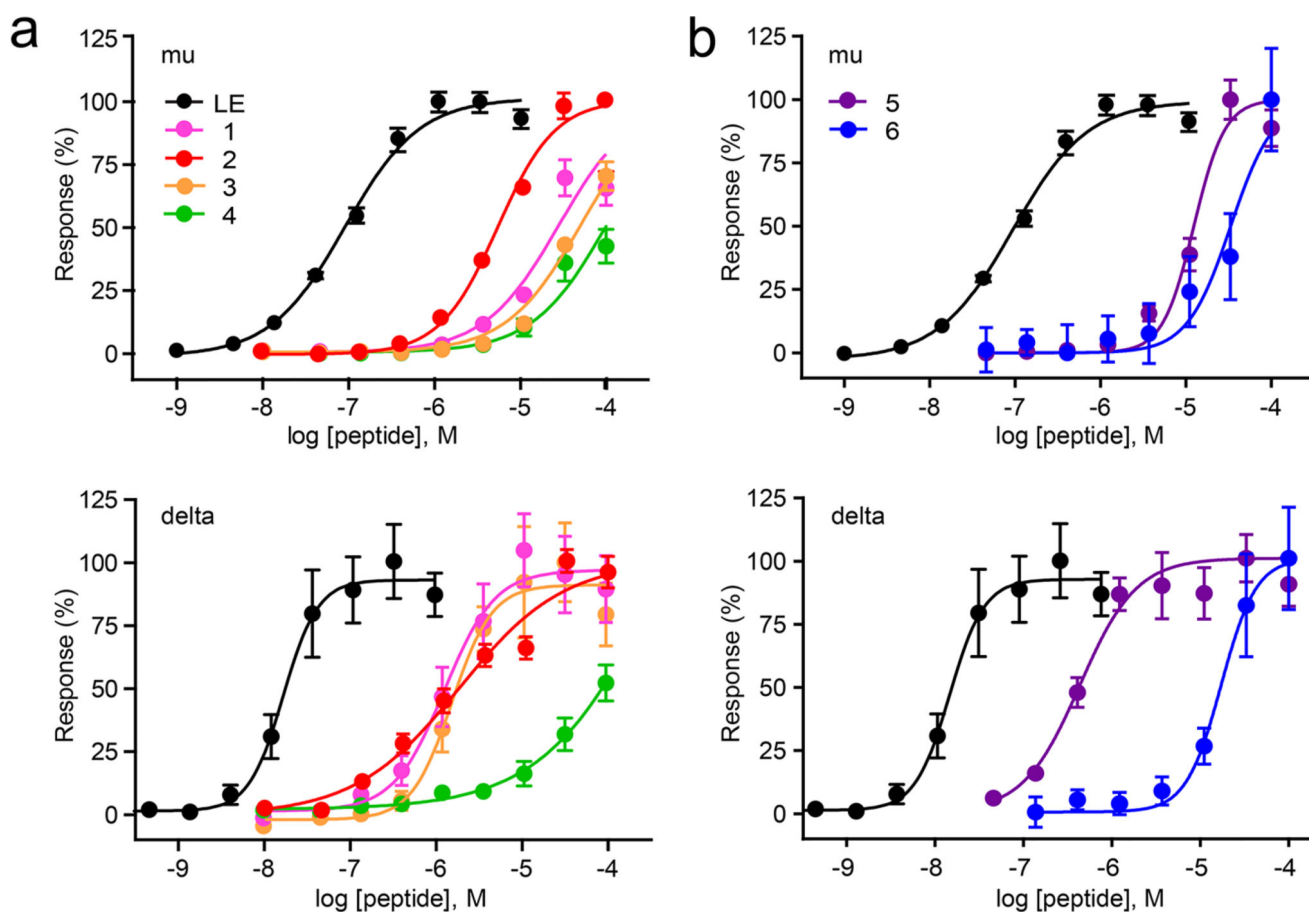
21. Corrie JE, DeSantis A, Katayama Y, Khodakhah K, Messenger JB, Ogden DC, Trentham DR. Postsynaptic activation at the squid giant synapse by photolytic release of L-glutamate from a “caged” L-glutamate. *J. Physiol.* 1993; 465:1–8. [PubMed: 7901400]

Author Manuscript

Author Manuscript

Author Manuscript

Author Manuscript

**Figure 1.**

Residual activity of caged LE derivatives at recombinant MOR and DOR. (a) Dose–response curves for 1–4 in comparison to LE at MOR (top) and DOR (bottom) expressed in HEK293T cells using a functional secreted-alkaline phosphatase (SEAP) assay ($n = 6–12$ wells per data point). Data were normalized to the maximal response to LE and are expressed as the mean \pm SEM. (b) As in (a) for 5 and 6. The same LE data is presented in both graphs.

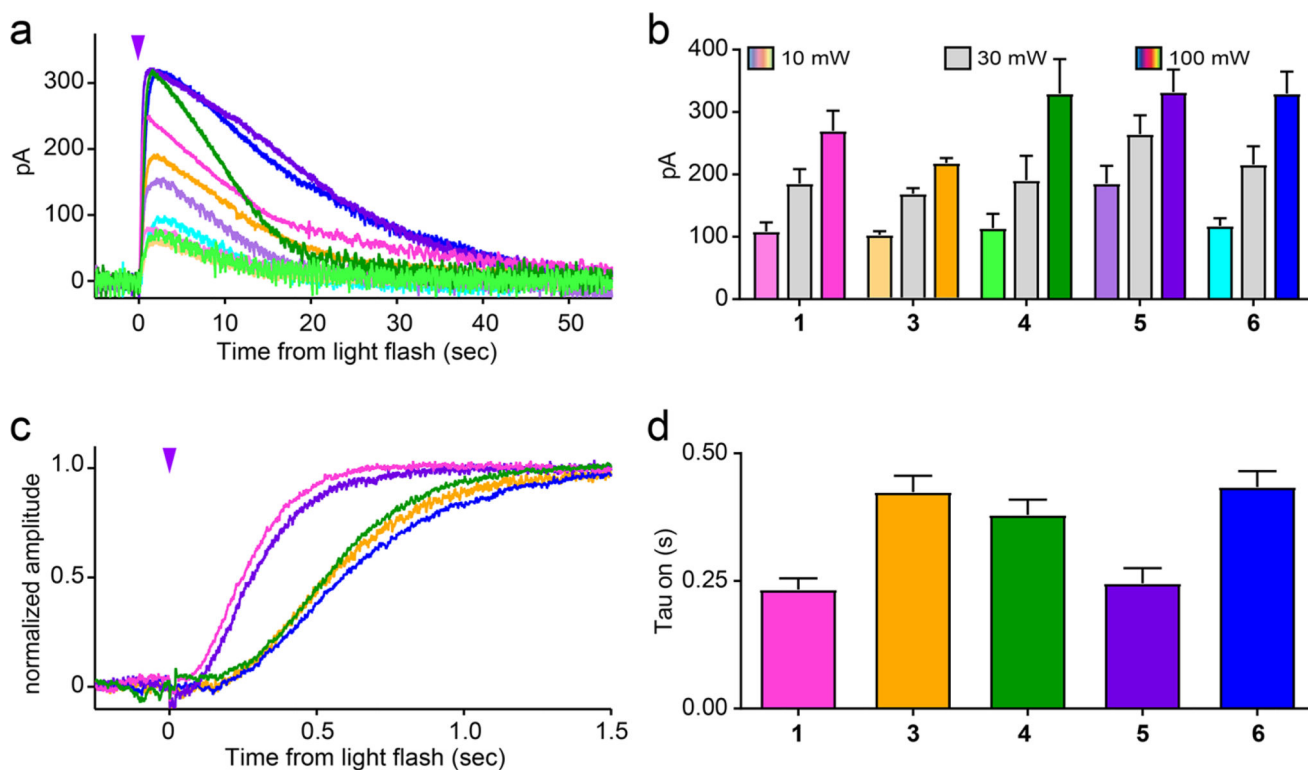
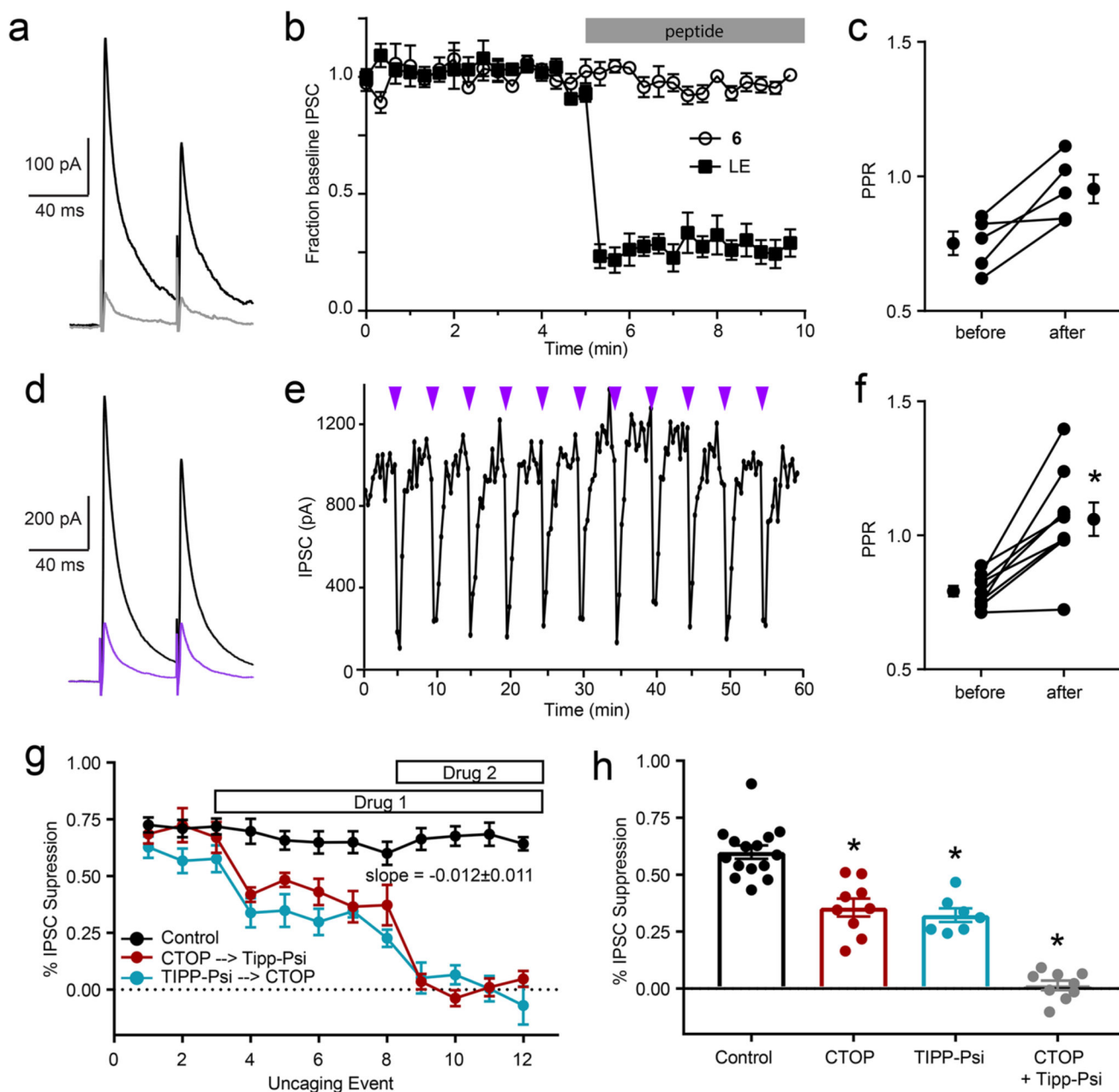
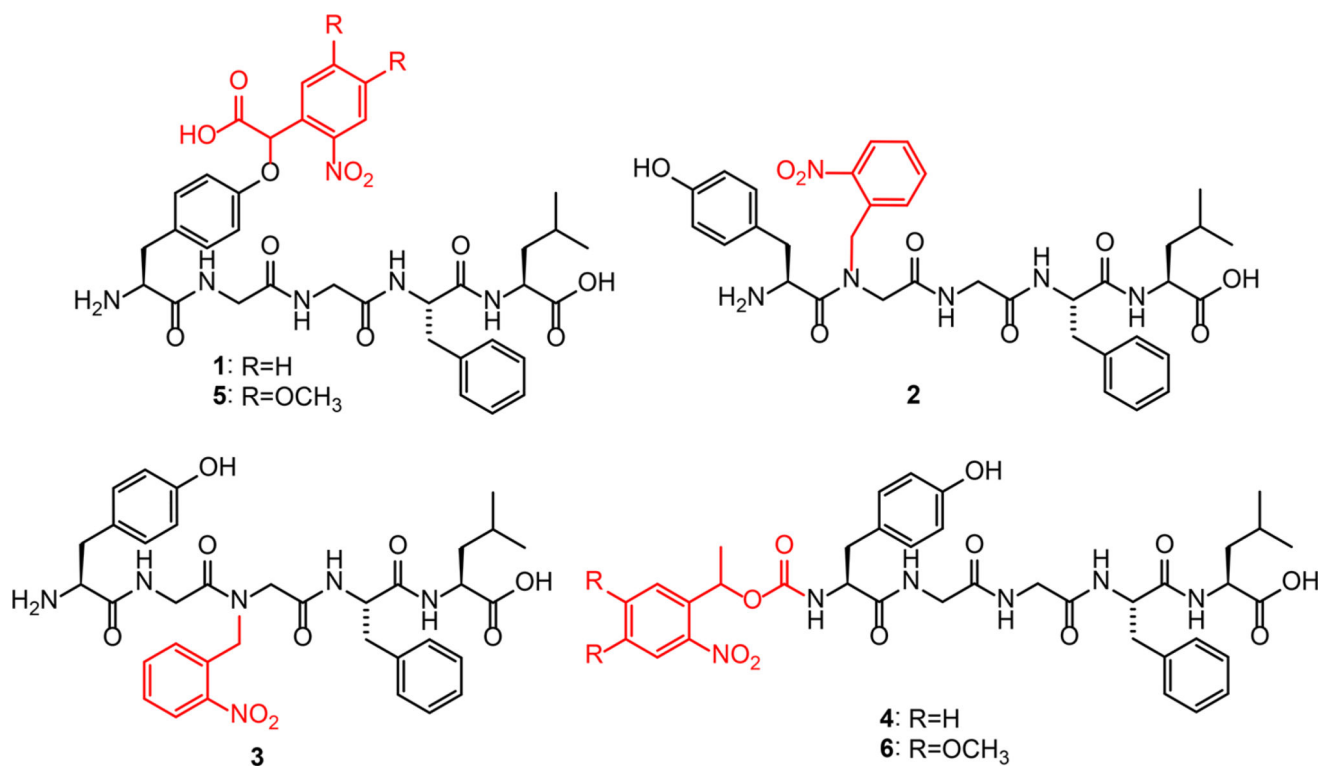


Figure 2. Functional analysis of light sensitivity and photorelease kinetics in brain slices of rat locus coeruleus. (a) Potassium currents evoked by photolysis at 10 μ M using a 50 ms flash of 10 or 100 mW 355 nm laser light. The traces shown are the average currents measured across multiple cells ($n = 6-9$ cells). Light flashes are indicated by purple arrowheads. (b) Summary of current amplitudes evoked at different power levels expressed as the mean \pm SEM. (c) Rising phase of amplitude-normalized average currents evoked by 100 mW light flashes. (d) Summary of the current activation time constants expressed as the mean \pm SEM.

**Figure 3.**

Uncovering mixed actions of LE via MOR and DOR on synaptic inhibition with *N*-MNVOC-LE (**6**) in brain slices of mouse hippocampus. (a) Electrically evoked inhibitory postsynaptic currents (IPSCs) in a pyramidal cell immediately before (black) and 3–5 min after (gray) bath application of LE (6 μ M). The traces shown are averages across 6 sweeps in a single cell. Two stimuli were applied with a 50 ms interstimulus interval. (b) Average baseline-normalized IPSC amplitude over time in response to bath application of LE ($n = 5$ cells) or **6** ($n = 9$ cells). (c) Summary of paired-pulse ratios (PPRs) measured before and after LE application. Each point represents the average across six sweeps in a single cell ($p = 0.0625$, Wilcoxon paired signed rank test). (d) IPSCs in a pyramidal cell immediately before

(black) and after (purple) photolysis of **6** (6 μM) using a 50 ms flash of light from a 365 nm LED. The traces shown are averages across 11 trials in a single cell. (e) IPSC amplitude over time measured in the same cell shown in panel (d). Light flashes were applied every 5 min. The amplitude of the first IPSC of the pair is shown. (f) Summary of paired-pulse ratios (PPRs) measured immediately before and after photolysis. Each point represents the average PPR measured across trials in a single cell ($n = 3\text{--}9$ trials per cell). Asterisk (*) denotes $p < 0.05$ (Wilcoxon paired signed rank test). (g) Photolysis-induced IPSC suppression over time in the absence and presence of highly specific opioid receptor antagonists. After three baseline uncaging events, either the MOR antagonist CTOP (1 μM , $n = 5$ cells) or the DOR antagonist TIPP-Psi (1 μM , $n = 5$ cells) was added to the bath (drug 1), followed by the other antagonist (drug 2). The indicated slope corresponds to a line fit to the antagonist-free control data set ($n = 9$ cells). (h) Summary of the photolysis-induced IPSC suppression data. In addition to the data shown in (g), cells are included for which only one drug was applied. Asterisks (*) denote $p < 0.05$ in comparison to control (Mann–Whitney U test).

**Scheme 1.**Caged Leucine-Enkephalin Derivatives^a

^aChemical structures of CYLE (1), *N*-NB-Gly²-LE (2), *N*-NB-Gly³-LE (3), *N*-NPEOC-LE (4), CNV-Y-LE (5), and *N*-MNVOC-LE (6). The caging groups are indicated in red.

Table 1

Summary of the Pharmacological Properties of Caged Enkephalin Derivatives

peptide	EC ₅₀ (M)	
	MOR	DOR
LE	6.50×10^{-7}	1.70×10^{-8}
1	4.80×10^{-5}	1.59×10^{-6}
2	5.67×10^{-6}	1.85×10^{-6}
3	2.89×10^{-5}	1.29×10^{-6}
4	1.25×10^{-4}	4.27×10^{-4}
5	1.24×10^{-5}	4.37×10^{-7}
6	3.35×10^{-5}	1.73×10^{-5}

Author Manuscript

Author Manuscript

Author Manuscript

Author Manuscript